Articles in PresS. J Appl Physiol (July 24, 2008). doi:10.1152/japplphysiol.90461.2008

NEUROMECHANICAL CONTROL OF THE ISOLATED UPPER AIRWAY OF MICE

Audrey Liu, MD
Luis Pichard, MHS
Hartmut Schneider, MD PhD
Susheel P. Patil, MD PhD
Philip L. Smith, MD
Vsevolod Polotsky, MD
Alan R. Schwartz, MD

Johns Hopkins Sleep Disorders Center, Division of Pulmonary and Critical Care Medicine, Johns Hopkins School of Medicine, Baltimore, MD 21224

Corresponding author:

Alan R. Schwartz, MD
Johns Hopkins Sleep Disorders Center
5501 Hopkins Bayview Circle
Baltimore, Maryland 21224 USA
Email: **aschwar2@jhmi.edu**
Tel: +001 (410) 550-0572
Fax: +001 (410) 550-3374

Supported by NIH HL50381 and HL37379

Running Head: Murine Upper Airway

ABSTRACT

We characterized the passive structural and active neuromuscular control of pharyngeal collapsibility in mice, and hypothesized that pharyngeal collapsibility, which is elevated by anatomic loads, is reduced by active neuromuscular responses to airflow obstruction. To address this hypothesis, we examined the dynamic control of upper airway function in the isolated upper airway of anesthetized C57BL/6J mice. Pressures were lowered downstream and upstream to the upper airway to induce inspiratory airflow limitation and critical closure of the upper airway, respectively. After hyperventilating the mice to central apnea, we demonstrated a critical closing pressure (Pcrit) of -6.2$\pm$1.1 cmH_2O under passive conditions that was unaltered by the state of lung inflation. After a period of central apnea, lower airway occlusion led to progressive increases in phasic genioglossal electromyographic activity (EMG_{GG}), and in maximal inspiratory airflow ($V_I max$) through the isolated upper airway, particularly as the nasal pressure was lowered toward the passive Pcrit level. Moreover, the active Pcrit fell during inspiration by 8.2±1.4 cmH_2O relative to the passive condition ($p<0.0005$). We conclude that upper airway collapsibility (passive Pcrit) in the C57BL/6J mouse is similar to that in the anesthetized canine, feline and sleeping human upper airway, and that collapsibility falls markedly under active conditions. Active EMG_{GG} and $V_I max$ responses dissociated at higher upstream pressure levels, suggesting a decrease in the mechanical efficiency of upper airway dilators. Our findings in mice imply that anatomic and neuromuscular factors interact dynamically to modulate upper airway function, and provide a novel approach to modeling the impact of genetic and environmental factors in inbred murine strains.

INTRODUCTION

Obstructive sleep apnea is a common disorder with a wide spectrum of neurocognitive, metabolic and cardiovascular consequences (28; 37; 39; 52; 61). Its clinical sequelae stem from frequent nocturnal arousals and/or oxyhemoglobin desaturations, which result from recurrent episodes of upper airway obstruction during sleep (41). Obstruction has been related to elevations in pharyngeal collapsibility during sleep (12; 36; 47; 53), although the mechanism for these elevations is not well understood.

Structural alterations and disturbances in neuromuscular control account for elevations in upper airway collapsibility in sleep apnea patients compared to normal controls (36). Boney and soft tissue defects can increase pharyngeal collapsibility by elevating the pressure in tissues around the pharynx (15-19; 59). The impact of structural alterations on upper airway collapsibility may be mitigated by increases in lung volume and caudal traction on upper airway structures (18; 42; 54-56), which decreases extraluminal tissue pressures (18) and/or stiffens the pharynx (42; 54). Neuromuscular responses to negative intraluminal pressures (25; 26), pulmonary mechanoreceptors and disturbances in gas exchange (43; 49; 51) can also lower upper airway collapsibility and relieve the obstruction during sleep (36). Thus, both structural and neuromuscular factors can modulate upper airway collapsibility during sleep (36) and contribute to the development of obstructive sleep apnea (7; 60).

Animal models have been developed to explore the impact of structural and neuromuscular factors on upper airway collapsibility. In isolated canine, feline, rat and rabbit upper airway preparations, the mechanical effects of lingual displacement, tracheal traction and extraluminal

tissue pressure (18-20; 42; 42; 54; 56) and the neuromuscular effects of alterations in gas exchange and airway pressure (1; 6; 8-10; 43; 51) on pharyngeal collapsibility have been demonstrated. Studies in pigs and bulldogs highlight the impact of structural narrowing on upper airway patency, particularly when neuromuscular activity wanes during REM sleep (14; 24; 58). Recently, investigators have demonstrated that obesity can also impose structural loads on the airway (5) that elevate pharyngeal collapsibility in the *fa/fa* rat, and that serotonergic mechanisms can offset this mechanical effect (27). We have demonstrated that a similar defect in leptin signaling in obese *ob/ob* mice accounts for the development of the obesity-hypoventilation syndrome in a murine model (29; 38), suggesting that mouse strains may ultimately serve to probe the genetic determinants of sleep related breathing disorders. Nevertheless, a mouse model of upper airway function will be required to explore the genetic control of pharyngeal collapsibility.

The primary objective of the present study was to characterize the passive structural and active neuromuscular control of upper airway collapsibility in mice. We hypothesized that pharyngeal collapsibility, which is elevated by anatomic/structural loads, is reduced by active neuromuscular responses to airflow obstruction. To address this hypothesis, we developed an approach for assessing upper airway mechanical and neuromuscular control in the isolated upper airway of anesthetized mice. Our findings provide new evidence that mechanical loads and neuromuscular mechanisms interact to control upper airway collapsibility dynamically, and offer an approach for probing genetic and environmental determinants of pharyngeal function in inbred muring strains.

METHODS

Mice

Male C57/BL6J mice were obtained from Jackson Laboratory (Bar Harbor, ME) and housed in a micro-isolation facility. Temperature and humidity were continuously regulated at 20-22^{o}C and 40-60% relative humidity, respectively. Food and water were available ad libitum throughout the study. Male mice were utilized exclusively to minimize any variability in upper airway characteristics related to the estrous cycle. All study protocols were approved by the Johns Hopkins Animal Care and Use Committee (JHACUC), and all animal experiments were conducted in accordance with JHACUC guidelines.

Experimental Procedures

Anesthesia Protocol: The murine upper airway was isolated as previously described for larger animals (49; 50). Briefly, surgical anesthesia was induced with 2-3% isoflurane in a closed chamber, and was maintained with urethane (1g/kg i.p.) and etomidate (10mg/kg i.p.) (11). Respiratory rate was continuously monitored, and additional doses of urethane, (0.2g/kg i.p.) and etomidate (2mg/kg i.p.) were administered as required to maintain a stable plane of surgical anesthesia. The depth of anesthesia was continuously monitored based on a targeted respiratory rate of 120-160 breaths/minute, and the absence of pedal withdrawal to interdigital space pinch. At experiment completion, the animals were euthanized by an overdose of pentobarbital (60mg i.p.). The rectal temperature was monitored continuously with a temperature probe, and body

temperature was maintained at 36.5-37.5°C with a variable temperature heating pad throughout the experiments.

Isolated Murine Upper Airway Surgery: Mice were instrumented with pressure catheters at the trachea and the nose as previously described (**Figure 1**) (49; 50). In brief, a midline neck incision from the sternum to the larynx was made while the mouse was supine. The trachea was transected, and the esophagus was ligated. Curved stainless steel 19 gauge catheters were placed in the caudal tracheal stub toward the lungs, and through the rostral tracheal stub and glottic structures to the level of the aryepiglottic folds, where it was fixed in place. The mice were mechanically ventilated through the caudal tracheal catheter (Harvard Instruments, Model 683, Holliston, MA). The rostral upper airway catheter was connected in series to a pneumotachometer and negative pressure source, which was utilized to maintain a negative pressure downstream in the hypopharynx (P_{DS}). One nostril was cannulated (27 gauge PE tubing). The mouth was sewn shut with 6-0 silk, and the mouth and nostrils were sealed with glue and putty. The cannulated nostril was utilized to deliver a variable upstream pressure at the nose (P_{US}). The position of the rostral tracheal cannula was confirmed to be at the level of the glottic opening at the conclusion of the experiment. In all experiments, the head was fixed in place at an angle of 10-20° from the horizontal plane.

Monitoring Pressure-Flow Dynamics: The upstream nasal (P_{US}) and downstream hypopharyngeal (P_{DS}) pressures were monitored (P23XL; Statham Laboratories), and inspiratory airflow (V_I) through the isolated upper airway was monitored with a pneumotachometer (No. 0.771, Fleisch, Switzerland) and a differential pressure transducer (Validyne, Northridge, CA; MP 45-1; ±2 cm H_2O). The pneumotachometer was calibrated by applying steady-state levels of

through a mass flow meter (Model FMA-A2303, Omega Engineering, Inc., Stamford, CT). The upstream nasal cannula was connected to a blow-by circuit that was attached on either side to a positive and negative pressure source. The pressure sources were regulated separately in order to apply varying levels of positive and negative pressure to the nose. The downstream tracheal cannula was connected to a negative pressure source. The P_{US}, P_{DS}, and V_I were digitized (WinDaq DI-720; DATAQ Instruments, Akron, OH) for real-time display and storage, and for later analysis. Throughout the experiments, secretions inside the catheter were flushed and aspirated through the catheter as needed.

Electromyography (EMG): Two Teflon-insulated hooked wire EMG electrodes (stainless steel wire, 0.005" bare, 0.007" coated, A-M Systems, Inc., Carlsborg, WA) were inserted using separate 26 gauge needles into the genioglossus muscle group bilaterally. The genioglossal EMG (EMG_{GG}) signal were amplified, band-pass-filtered from 30 to 1,000 Hz (P511K, AC Pre-amplifier, Grass Instruments Co., Quincy, MA), and digitized at a sampling rate of 1,000 Hz (WinDaq DI-720; DATAQ Instruments, Akron, OH). The EMG_{GG} was rectified and a 200 milliseconds time constant was utilized to compute the moving average (Advanced Codas, DATAQ Instruments). The moving average was employed for all subsequent data analysis (see below).

Mechanical Ventilation: Mice were mechanically ventilated through the caudal tracheal tube with a tidal volume of approximately 200µL and respiratory rate of 120-140 breaths per minute (Model 687 Small Animal Ventilator, Harvard Apparatus, Inc., Holliston, MA). Respiratory rate was adjusted to induce a passive state for the pharyngeal musculature by suppressing phasic EMG_{GG} activity and spontaneous respiration (as assessed by negative tracheal pressure swings).

Positive end-expiratory pressure (PEEP) was applied at the exhalation port (0, 5 and 10 cmH_2O) as described in *protocol* below. Prior to each passive and active run (see *Protocols* below), the tidal volume and respiratory rate were increased to approximately 250μL and 180 breaths per minute, respectively, to induce a period of central apnea. The mouse was hyperventilated for several minutes prior to passive runs or for ~15 seconds prior to active runs in order to induce relatively prolonged or short periods of central apnea when mechanical ventilation was discontinued.

Experimental Protocol

Characterizing Passive Upper Airway Properties: Initially, P_{DS} was lowered to ~-50 cmH_2O to induce a flow-limited state for the upper airway, as defined by a plateau in V_I at a maximal level ($V_I$max) despite further reductions in P_{DS} (42; 43; 48; 49; 51; 54). Thereafter, the level of airflow ($V_I$max) through the isolated upper airway was determined at several P_{US} levels. At each P_{US} level, mechanical ventilation was discontinued in order to maintain a constant lung volume when measuring $V_I$max during the ensuing central apnea. P_{US} was lowered to defined levels of 4, 0, -4, -8 cmH_2O in successive runs to encompass the level of nasal pressure at which flow ceased (the pharynx occluded when P_{US} fell below a critical pressure). At each level of P_{US}, $V_I$max was measured at a PEEP of 0, 5 and 10 cmH_2O to determine the effect of lung inflation on upper airway properties. Runs at each level of P_{US} were performed in triplicate in the passive and active protocols (see below).

Characterizing Active Upper Airway Properties: As in the *passive protocol*, P_{DS} was lowered to induce a flow-limited state, as defined above. Mechanical ventilation was discontinued and the

caudal tracheal cannula was occluded for ~10 seconds, or until a sigh or swallow occurred. Following a brief period of central apnea, spontaneous breathing resumed and inspiratory efforts increased progressively. Peak phasic and tonic levels of $V_I$max and EMG_{GG} were monitored throughout the period of tracheal occlusion during inspiration and expiration, respectively. Tracheal occlusion led to progressive increases in inspiratory effort (P_{TRACH}), $V_I$max and EMG_{GG} from the start to end of the run. Active responses to tracheal occlusion were characterized by the changes in $V_I$max and EMG_{GG} over the course of each run (as described in *Results, Figure 4)*. The tracheostomy was then reopened, and mechanical ventilation was resumed until spontaneous respiratory efforts and phasic EMG_{GG} abated. The nasal pressure was lowered in step-wise fashion, and active runs were repeated at P_{US} levels as described above (*see passive protocol*). During active runs, the trachea was occluded for 9.9 ± 1.3 seconds across all nasal pressure levels and mice.

Data Analysis

In the passive protocol, $V_I$max and P_{US} were measured during periods of central apnea, and separate pressure-flow relationships were constructed at each PEEP level. In the active protocol, $V_I$max and EMG_{GG} responses to tracheal occlusion were assessed at each level of P_{US}. These parameters were measured repeatedly for each inspiration and expiration during the entire run. The maximal EMG_{GG} activity was measured for each active (tracheal occlusion) run and the mean maximal activity was calculated for each mouse. Subsequently, the peak phasic and tonic (minimum) levels of EMG_{GG} were measured for each inspiration and expiration, respectively, and were expressed as a percentage of the mean maximal EMG_{GG} activity in each mouse. Least squares linear regression was utilized to characterize the rate of increase in EMG_{GG} and $V_I$max

over time during periods of tracheal occlusion. To examine the phasic control of pharyngeal patency during periods of tracheal occlusion, phasic responses were represented as changes in $V_I$max (ΔV_Imax) and EMG_{GG} (ΔEMG_{GG}) by subtracting the corresponding level of $V_I$max and EMG_{GG} activity during the preceding central apnea from phasic and tonic levels of these parameters during the period of spontaneous breathing (see Figure 5).

Separate pressure-flow relationships were constructed from data generated at each of several P_{US} levels (between 10 and 30 points in total) in both the passive and active protocols. Least squares linear regression was applied over the linear portion of each $V_I$max vs. P_{US} relationship to determine the critical pressure (Pcrit) and upstream resistance (R_{US}), as previously described (36). In the active protocol, a passive $V_I$max vs. P_{US} relationship was constructed from data obtained at the start of each run (before neuromuscular activation), from which the passive Pcrit and R_{US} were derived. Pressure-flow data from the point of maximal neuromuscular activation at the end of each run were utilized to generate a separate *active* pressure-flow relationship. Neuromuscular modulation of upper airway function was quantified as the degree of leftward displacement of the active curve from the passive pressure-flow relationship at the passive Pcrit level. This pressure difference between the active and passive curves at the passive Pcrit level (ΔP_{A-P}) was taken to be a measure of the strength of the neuromuscular response (36). The sum of the passive Pcrit and the pressure difference, ΔP_{A-P}, was calculated in order to estimate the active Pcrit.

Values were expressed as mean ± SEM. Linear mixed-effects regression analysis (XTMIXED, Intercooled Stata 9.2, Statacorp, College Station, TX) was utilized to model the effect of PEEP on Pcrit and R_{US} (passive protocol), the time course of responses in $V_I$max and peak phasic and

tonic EMG_{GG} to tracheal occlusion, and the effect of tracheal occlusion on Pcrit and R_{US} (active protocol). When significant differences were detected, post-hoc comparisons were performed (Tukey) to determine the source of these differences. Statistical significance was inferred at a $p<0.05$ level.

RESULTS

Passive upper airway properties

Upper airway passive properties were characterized in 6 mice (weight, 26.1 ± 1.8 g; age, 94.0 ± 4.1days). Representative P_{TRACH}, EMG_{GG}, and $V_I$max recordings are illustrated in one mouse at three levels of nasal pressure in separate panels (**Figure 2**), while a markedly negative pressure was maintained at the downstream end of the isolated upper airway to induce inspiratory airflow limitation. At each nasal pressure level, three levels of PEEP (0, 5, and 10 cmH_2O) were applied (**Figure 2**, see step changes in P_{TRACH} signals in each panel). At the start of each run in each panel, positive pressure ventilation was applied to the lower tracheostomy in order to hyperventilate the mouse (see positive P_{TRACH} swings from ventilator on left side of each panel). When the ventilator was stopped, a prolonged central apnea ensued (EMG_{GG} and P_{TRACH} remained quiescent for the remainder of the run, see right side of each panel). During this apnea, airflow through the isolated upper airway remained constant at each level of nasal pressure (see panels for each P_{US} level). As the nasal pressure was reduced from 4 to 0 to -4 cmH_2O, the level of airflow ($V_I$max) decreased progressively and ultimately ceased at the lowest nasal pressure applied (see left, center and right panels, respectively). Moreover, the level of $V_I$max remained constant as PEEP was increased step-wise from 0 to 5 and 10 cmH_2O at each nasal pressure

level, indicating no effect of lung inflation on upper airway flow. $V_I$max vs. P_{US} for the isolated upper airway in the representative mouse shown in **Figure 2** demonstrated a linear relationship with a passive Pcrit of -5.9 cmH_2O (**Figure 3**), and no influence of PEEP on this relationship.

In **Table 1**, passive Pcrit and R_{US} are reported at PEEP of 0, 5 and 10 cm H_2O for the entire group. The mean passive Pcrit was -6.19 ± 1.11 cmH_2O and R_{US} was 13.8 ± 1.8 cm H_2O/mL/s, and did not change significantly as a function of the level of PEEP.

Active upper airway properties during lower tracheal occlusion

Active responses to lower airway occlusion were assessed in a separate group of 7 mice (weight, 26.4 ± 0.8 g; age, 83.6 ± 11 days). Representative recordings are illustrated for one mouse at -4.0 cm H_2O and 0.0 cm H_2O level of nasal pressure (**Figure 4**, left and right panels, respectively). As in the passive protocol, P_{DS} was lowered to induce a flow-limited state for the isolated upper airway, and positive pressure ventilation was applied to the lower airway (see augmenting positive P_{TRACH} swings on left side of panels). After discontinuing mechanical ventilation, an initial period of central apnea was followed by a progressive increase in inspiratory efforts (see negative P_{TRACH} swings in middle and right half of each panel, **Figure 4**). At the start of the run (T_O), baseline levels of airflow through the isolated upper airway were greater at a high (~1.1 mL/s) compared to low (~0.6 mL/s) nasal pressure level, as expected. As tracheal pressure swings increased, phasic changes in EMG_{GG} and airflow ensued and increased progressively over time (see Flow and EMG_{GG} vs. time, two lower signals, **Figure 4**). Comparing EMG_{GG} responses to tracheal occlusion at high and low nasal pressures, we found that levels of tonic EMG_{GG} were similar at the start and end of these runs (at T_O and T_f), and that

phasic EMG_{GG} activity increased similarly over time. By the end of the run (T_f), phasic changes in airflow were greater at the low compared to high nasal pressure level (**Figure 4,** left vs. right panel).

As illustrated in **Figure 4** (lower graphs), the peak phasic (inspiratory) and tonic (expiratory) EMG_{GG} and $V_I$max rose linearly over time in each mouse during periods of tracheal occlusion ($p<0.0003$). The rate of rise in $V_I$max was significantly greater during inspiration than expiration (3.18 ± 0.67 vs. 1.25 ± 0.30mL/s/s, $p<0.003$), as was the rate of rise in EMG_{GG} (0 0.06 ± 0.01 vs..01 $\pm$ 0.003 μV/s, $p <0.0001$). Since $V_I$max and EMG_{GG} increased linearly over time during periods of tracheal occlusion, the initial and final breaths of each run were utilized to examine the neuromuscular control of upper airway patency over the range of upstream pressures applied.

In **Figure 5**, the relationship between changes in $V_I$max and EMG_{GG} are illustrated for the highest and lowest levels of P_{US} applied (Low P_{US}: -3.4±1.1; High P_{US}: 5.7± 0.6 cmH_2O). Despite comparable increases in EMG_{GG} during tracheal occlusion over the entire range of P_{US} applied, $V_I$max increased markedly only at the low ($p<0.001$) but not high P_{US} level.

In **Figure 6**, the effects of tracheal occlusion on the passive and active pressure-flow relationships are illustrated for the mouse whose recording examples appear in **Figure 4**. $V_I$max at two levels of P_{US} are plotted for data obtained from the start of the run, demonstrating a passive Pcrit of -4.2 cm H_2O. During tracheal occlusion, peak inspiratory $V_I$max increased by the end of the run (see **Figure 4**) more at the lower compared to higher level of P_{US}, decreasing the slope of the active compared to passive pressure-flow relationship (see *Active curve,* **Figure 6**). The shift in the active pressure-flow relationship from the passive curve, ΔP_{A-P}, provided a

measure of the strength of neuromuscular activation at the passive Pcrit level, as shown. Utilizing ΔP_{A-P} to estimate the active Pcrit (see Methods), we found significant decreases in Pcrit and increases in R_{US} at maximum activation during inspiration compared to expiration, and compared to the passive condition at the onset of tracheal occlusion for the entire group (**Figure 7**). Compared to the passive pressure-flow relationship, the active curve was displaced leftward and reduced in slope, leading to underestimates of the active Pcrit (as represented by the nasal pressure at zero flow) and the Pcrit response to tracheal occlusion. The passive Pcrit did not differ significantly in the active compared to the passive protocol (p = n.s.).

DISCUSSION

In this study, we examined the mechanical and neuromuscular control of pharyngeal collapsibility in the isolated upper airway of the mouse. Passive pressure-flow relationships demonstrated a moderately negative passive Pcrit in the range previously found in sleeping humans (2; 35; 36; 45). In contrast to studies in larger mammals and human, the passive Pcrit did not vary with alterations in lung volume (PEEP), suggesting that it was primarily determined by pharyngeal soft tissues and boney structures. These passive properties were modulated dynamically by tracheal occlusion, which elicited progressive neuromuscular responses in phasic genioglossal activity and upper airway flow. Of note, responses in airflow were most marked at low compared to high levels of nasal pressure, leading to a reduced slope of the pressure-flow relationship with a concomitant decrease in active Pcrit and increase in R_{US} compared to passive conditions. In contrast, EMG_{GG} responses to tracheal occlusion did not vary with nasal pressure, and were only associated with substantial phasic increases in airflow at lower levels of nasal pressure. These differences in EMG_{GG} and airflow responses can be attributed to improved

neuromechanical coupling when the pharyngeal transmural pressure is reduced. Our findings imply that passive and active elements interact dynamically to modulate the collapsibility of the isolated murine upper airway, and establish an approach for modeling the impact of these components on sleep apnea susceptibility.

Our approach to modeling murine upper airway function under passive conditions was based on principles of pressure-flow dynamics in simple collapsible conduits (Starling resistor). The isolated murine upper airway demonstrated two essential characteristics of a Starling resistor (46; 47; 53). First, inspiratory airflow limitation was produced by lowering the downstream (tracheal) pressure until airflow plateaued at a maximal level ($V_I$max) and became independent of further decreases in downstream pressure. Second, maximal inspiratory airflow ($V_I$max) was linearly related to the upstream (nasal) pressure, and ceased when nasal pressure fell below a critical pressure, as described for sleeping humans. Pcrit and R_{US} for the isolated murine upper airway were derived from the $V_I$max vs. P_{US} relationship. In contrast to previous methods for assessing these parameters in larger animals (1; 8-10; 27; 30; 40), the current approach obviated the need for an intraluminal pressure-monitoring cannula in the pharynx, which might have produced artifactual changes in our measurements of upper airway properties in the mouse. Despite this methodologic difference, pressure-flow dynamics in the isolated murine upper airway resembled those previously demonstrated in the larger anesthetized animals and sleeping humans and yielded comparable levels of passive Pcrit (27; 30; 46; 47; 49; 51; 53), suggesting similarities in the mechanical determinants of pharyngeal patency.

The passive Pcrit can be modulated by pharyngeal tissue pressure (rabbit) and caudal traction (dog, cat) on upper airway structures (13; 42; 50). The latter is produced by elevations in lung

volume and transmitted by mechanical attachments between the chest and upper airway structures (55; 56). In contrast to prior studies in larger animals and humans, PEEP, a surrogate for increasing lung volume in our preparation, did not influence the passive Pcrit in our isolated murine upper airway. This finding suggests that mechanical linkage between chest and upper airway structures is lacking in this murine model. Such linkage may be diminished by the elevated compliance of the murine chest wall (23), or by fixing the position of the rostral tracheal stump in our preparation (54). While lung volume can still influence upper airway function in dogs even when the tracheal position is fixed (56), our findings in the murine upper airway suggest that pharyngeal collapsibility under passive conditions is largely determined by upper airway rather than thoraco-cervical structures.

Relative to passive conditions, tracheal occlusion elicited progressive increases in phasic genioglossal activity over the entire range of upstream pressures applied, although phasic increases in upper airway flow were only observed at lower levels of upstream nasal pressure. These responses can be attributed to a loss of phasic inhibition from pulmonary mechanoreceptor and progressive disturbances in gas exchange (51), leading to marked increases in pharyngeal neuromuscular activity (49). Our methods allowed us to quantify the strength of the pharyngeal musculature by referencing active responses to the passive state. In the passive condition, the pharynx occluded when the nasal pressure was lowered to the passive Pcrit level, at which point the pharyngeal transmural pressure became zero. At this level of nasal pressure, any increase in airflow in the active condition could be attributed to increased dilator activity (31; 33; 34; 44; 50), which can decrease the extraluminal tissue pressure (19) and increase transmural pressure accordingly. Alternatively, airway patency may have been stabilized by co-activation of tongue protrusor and retrusor muscles (1; 8-10), pharyngeal constrictors (22), and/or cervical strap

muscles (33; 57). Thus, the pressure difference between the active and passive curve is caused by differences in transmural pressure, and may reflect the strength of pharyngeal dilator and constrictor muscles, tongue protrusor and retrusor muscle and/or cervical strap muscle responses to tracheal occlusion. Differences in airflow responses to tracheal occlusion at the passive Pcrit level suggest that the mechanical efficiency of the pharyngeal musculature increases as the upstream pressure is lowered. Nevertheless, measurements of muscle force during tracheal occlusion would be required to confirm this conclusion.

An intriguing finding was that in contrast to EMG_{GG} responses to tracheal occlusion, phasic changes in airflow increased progressively with reductions in nasal pressure. Responses in airflow and neuromuscular activity dissociated at higher nasal pressures, suggesting a loss of dilating action in pharyngeal muscles (see **Figure 8**). The mechanical efficiency of these dilator muscles depends on their resting length (3; 4; 32), which may vary with the size of the pharyngeal lumen relative to its boney enclosure (59). At lower levels of nasal pressure, the pharynx will narrow, and dilators will elongate toward their optimal length (L_O) (32). Neuromuscular activation at L_O would yield the greatest increase in tension, transmural pressure and airflow. Alternatively, overdistension of the pharyngeal lumen relative to the size of the boney enclosure (21; 59) may limit the mechanical action of these dilating muscles.

Several limitations should be considered when interpreting our data. First, our approach to characterizing the passive and active properties of the upper airway requires that a flow-limited state be achieved by lowering the downstream tracheal pressure below inspiratory levels. This downstream pressure was confined to the hypopharynx, and exposure was limited in duration in order to avoid mucosa drying. Second, active responses were assessed over a relatively narrow

range of nasal pressures that were applied to define the passive pressure-flow relationship. Nevertheless, our protocol elicited a marked neuromuscular response and allowed us to isolate the active component of this response from the passive baseline (36). Third, we recognize that dynamic responses during anesthesia cannot be extrapolated to sleep. Nonetheless, the isolated murine upper airway exhibited pressure-flow dynamics, a passive Pcrit, and dynamic neuromuscular responses that were remarkably similar to those previously demonstrated across species (27; 30; 43; 49; 51) and in sleeping subjects (36). Despite differences in upper airway anatomy and size, it is nonetheless remarkable that inspiratory airflow limitation and critical closure occur at similar levels of pharyngeal critical pressure in normal sleeping humans and in anesthetized dogs, rabbits, cats, rats and mice (10; 27; 42; 49; 51; 54). Finally, we recognize that our genioglossal EMG signal may have included activity from adjacent intrinsic tongue muscles, dilator muscles (e.g., geniohyoid), tongue retrusors (e.g. stylohyoid and geniohyoid) and cervical strap muscles due to close proximity of these muscles to the recording electrodes.

Our approach to analyzing upper airway pressure-flow relationships under active and passive conditions has yielded new insights into mechanisms of upper airway neuromuscular control. In contrast to prior work in larger animals, our strategy for probing neuromuscular control mechanisms in mice was based on comparisons of pressure-flow dynamics over a range of upstream pressure. Utilizing this approach, we found evidence that active neuromuscular control of pharyngeal collapsibility is greatest at low levels of upstream (transmural) pressure. These findings suggest that the pharyngeal transmural pressure influences the mechanical efficiency of the musculature for any given level of neural output.

Our findings have also laid a foundation for studies examining the impact of genetic and environmental factors on murine upper airway control. They serve to establish a conceptual foundation for modeling passive and active upper airway properties across species. This experimental approach can be utilized to capitalize on the power of inbred murine strains to explore the genetic basis for alterations in upper airway control. In addition, inbred murine strains can be employed to examine the impact of environmental exposure on upper airway control (e.g., caloric excess leading to obesity, local pharyngeal inflammation and interactions with underlying cardiopulmonary disease). Finally, further work will be required to characterize and evaluate the impact of these factors on upper airway function during sleep.

ACKNOWLEDGEMENTS: We wish to acknowledge the technical expertise of Ahmed Elsayed-Ahmed.

Reference List

1. **Bailey EF and Fregosi RF**. Pressure-volume behaviour of the rat upper airway: effects of tongue muscle activation. *Journal of Physiology-London* 548: 563-568, 2003.

2. **Boudewyns A, Punjabi N, Van de Heyning PH, De Backer WA, O'Donnell CP, Schneider H, Smith PL and Schwartz AR**. Abbreviated Method for Assessing Upper Airway Function in Obstructive Sleep Apnea. *Chest* 118: 1031-1041, 2000.

3. **Brennick MJ, Parisi RA and England SJ**. Influence of preload and afterload on genioglossus muscle length in awake goats. *Am J Respir Crit Care Med* 155: 2010-2017, 1997.

4. **Brennick MJ, Parisi RA and England SJ**. Genioglossal length and EMG responses to static upper airway pressures during hypercapnia in goats. *Respir Physiol* 127: 227-239, 2001.

5. **Brennick MJ, Pickup S, Cater JR and Kuna ST**. Phasic respiratory pharyngeal mechanics by magnetic resonance imaging in lean and obese zucker rats. *Am J Respir Crit Care Med* 173: 1031-1037, 2006.

6. **Brouillette RT and Thach BT**. Control of genioglossus muscle inspiratory activity. *J Appl Physiol* 49: 801-808, 1980.

7. **Eastwood PR, Szollosi I, Platt PR and Hillman DR**. Comparison of upper airway collapse during general anaesthesia and sleep. *Lancet* 359: 1207-1209, 2002.

8. **Fregosi RF and Fuller DD**. Respiratory-related control of extrinsic tongue muscle activity. *Respir Physiol* 110: 295-306, 1997.

9. **Fuller D, Mateika JH and Fregosi RF**. Co-activation of tongue protrudor and retractor muscles during chemoreceptor stimulation in the rat. *J Physiol (Lond)* 507: 265-276, 1998.

10. **Fuller D, Williams JS, Janssen PL and Fregosi RF**. Effect of co-activation of tongue protrudor and retractor muscles on tongue movements and pharyngeal airflow mechanics in the rat. *J Physiol (Lond)* 519 Pt 2:601-13: 601-613, 1999.

11. **Georgakopoulos D and Kass D**. Minimal force-frequency modulation of inotropy and relaxation of in situ murine heart. *J Physiol* 534: 535-545, 2001.

12. **Gleadhill IC, Schwartz AR, Schubert N, Wise RA, Permutt S and Smith PL**. Upper airway collapsibility in snorers and in patients with obstructive hypopnea and apnea. *Am Rev Respir Dis* 143: 1300-1303, 1991.

13. **Gold AR and Schwartz AR**. The pharyngeal critical pressure. The whys and hows of using nasal continuous positive airway pressure diagnostically. *Chest* 110: 1077-1088, 1996.

14. **Hendricks JC, Kline LR, Kovalski RJ, O'Brien JA, Morrison AR and Pack AI**. The English bulldog: a natural model of sleep-disordered breathing. *J Appl Physiol* 63: 1344-1350, 1987.

15. **Isono S, Remmers JE, Tanaka A, Sho Y, Sato J and Nishino T**. Anatomy of the pharynx in patients with obstructive sleep apnea and in normal subjects. *J Appl Physiol* 82: 1319-1326, 1997.

16. **Isono S, Saeki N, Tanaka A and Nishino T**. Collapsibility of passive pharynx in patients with acromegaly. *Am J Respir Crit Care Med* 160: 64-68, 1999.

17. **Isono S, Tanaka A, Tagaito Y, Sho Y and Nishino T**. Pharyngeal patency in response to advancement of the mandible in obese anesthetized persons. *Anesthesiology* 87: 1055-1062, 1997.

18. **Kairaitis K, Byth K, Parikh R, Stavrinou R, Wheatley JR and Amis TC**. Tracheal traction effects on upper airway patency in rabbits: the role of tissue pressure. *Sleep* 30: 179-186, 2007.

19. **Kairaitis K, Parikh R, Stavrinou R, Garlick S, Kirkness JP, Wheatley JR and Amis TC**. Upper airway extraluminal tissue pressure fluctuations during breathing in rabbits. *J Appl Physiol* 2003.

20. **Koenig JS and Thach BT**. Effects of mass loading on the upper airway. *J Appl Physiol* 64: 2294-2299, 1988.

21. **Kuna ST and Brennick MJ**. Effects of pharyngeal muscle activation on airway pressure-area relationships. *Am J Respir Crit Care Med* 166: 972-977, 2002.

22. **Kuna ST and Vanoye CR**. Respiratory-related pharyngeal constrictor muscle activity in decerebrate cats. *J Appl Physiol* 83: 1588-1594, 1997.

23. **Lai YL and Chou H**. Respiratory mechanics and maximal expiratory flow in the anesthetized mouse. *J Appl Physiol* 88: 939-943, 2000.

24. **Lonergan RP, Ware JC, Atkinson RL, Winter WC and Suratt PM**. Sleep apnea in obese miniature pigs. *J Appl Physiol* 84: 531-536, 1998.

25. **Malhotra A, Fogel RB, Edwards JK, Shea SA and White DP**. Local mechanisms drive genioglossus activation in obstructive sleep apnea. *Am J Respir Crit Care Med* 161: 1746-1749, 2000.

26. **Malhotra A, Pillar G, Fogel RB, Beauregard J, Edwards JK, Slamowitz DI, Shea SA and White DP**. Genioglossal But Not Palatal Muscle Activity Relates Closely to Pharyngeal Pressure. *Am J Respir Crit Care Med* 162: 1058-1062, 2000.

27. **Nakano H, Magalang UJ, Lee SD, Krasney JA and Farkas GA**. Serotonergic modulation of ventilation and upper airway stability in obese Zucker rats. *Am J Respir Crit Care Med* 163: 1191-1197, 2001.

28. **Nieto FJ, Young TB, Lind BK, Shahar E, Samet JM, Redline S, D'Agostino RB, Newman AB, Lebowitz MD and Pickering TG**. Association of sleep-disordered breathing, sleep apnea, and hypertension in a large community-based study. Sleep Heart Health Study. *JAMA* 283: 1829-1836, 2000.

29. **O'Donnell CP, Schaub CD, Haines AS, Berkowitz DE, Tankersley CG, Schwartz AR and Smith PL**. Leptin prevents respiratory depression in obesity. *Am J Respir Crit Care Med* 159: 1477-1484, 1999.

30. **Ogasa T, Ray AD, Michlin CP, Farkas GA, Grant BJ and Magalang UJ**. Systemic administration of serotonin 2A/2C agonist improves upper airway stability in Zucker rats. *Am J Respir Crit Care Med* 170: 804-810, 2004.

31. **Oliven A, O'hearn DJ, Boudewyns A, Odeh M, De BW, Van de HP, Smith PL, Eisele DW, Allan L, Schneider H, Testerman R and Schwartz AR**. Upper airway response to electrical stimulation of the genioglossus in obstructive sleep apnea. *J Appl Physiol* 95: 2023-2029, 2003.

32. **Oliven A and Odeh M**. Effect of positional changes of anatomic structures on upper airway dilating muscle shortening during electro- and chemostimulation. *J Appl Physiol* 101: 745-751, 2006.

33. **Oliven A, Odeh M, Geitini L, Oliven R, Steinfeld U, Schwartz AR and Tov N**. Effect of co-activation of tongue protrusor and retractor muscles on pharyngeal lumen and airflow in sleep apnea patients. *J Appl Physiol* 2007.

34. **Oliven A, Tov N, Geitini L, Steinfeld U, Oliven R, Schwartz AR and Odeh M**. Effect of genioglossus contraction on pharyngeal lumen and airflow in sleep apnoea patients. *Eur Respir J* 30: 748-758, 2007.

35. **Patil SP, Punjabi NM, Schneider H, O'Donnell CP, Smith PL and Schwartz AR**. A simplified method for measuring critical pressures during sleep in the clinical setting. *Am J Respir Crit Care Med* 170: 86-93, 2004.

36. **Patil SP, Schneider H, Marx JJ, Gladmon E, Schwartz AR and Smith PL**. Neuromechanical control of upper airway patency during sleep. *J Appl Physiol* 102: 547-556, 2007.

37. **Peppard PE, Young T, Palta M and Skatrud J**. Prospective study of the association between sleep-disordered breathing and hypertension. *N Engl J Med* 342: 1378-1384, 2000.

38. **Polotsky VY, Wilson JA, Smaldone MC, Haines AS, Hurn PD, Tankersley CG, Smith PL, Schwartz AR and O'Donnell CP**. Female gender exacerbates respiratory depression in leptin-deficient obesity. *Am J Respir Crit Care Med* 164: 1470-1475, 2001.

39. **Punjabi NM, Sorkin JD, Katzel LI, Goldberg AP, Schwartz AR and Smith PL**. Sleep-disordered breathing and insulin resistance in middle-aged and overweight men. *Am J Respir Crit Care Med* 165: 677-682, 2002.

40. **Ray AD, Magalang UJ, Michlin CP, Ogasa T, Krasney JA, Gosselin LE and Farkas GA**. Intermittent hypoxia reduces upper airway stability in lean but not obese Zucker rats. *Am J Physiol Regul Integr Comp Physiol* 293: R372-R378, 2007.

41. **Remmers JE, deGroot WJ, Sauerland EK and Anch AM**. Pathogenesis of upper airway occlusion during sleep. *J Appl Physiol* 44: 931-938, 1978.

42. **Rowley JA, Permutt S, Willey S, Smith PL and Schwartz AR**. Effect of tracheal and tongue displacement on upper airway airflow dynamics. *J Appl Physiol* 80: 2171-2178, 1996.

43. **Rowley JA, Williams BC, Smith PL and Schwartz AR**. Neuromuscular activity and upper airway collapsibility. Mechanisms of action in the decerebrate cat. *Am J Respir Crit Care Med* 156: 515-521, 1997.

44. **Schwartz AR, Eisele DW, Hari A, Testerman R, Erickson D and Smith PL**. Electrical stimulation of the lingual musculature in obstructive sleep apnea. *J Appl Physiol* 81: 643-652, 1996.

45. **Schwartz AR, O'Donnell CP, Baron J, Schubert N, Alam D, Samadi SD and Smith PL**. The hypotonic upper airway in obstructive sleep apnea: role of structures and neuromuscular activity. *Am J Respir Crit Care Med* 157: 1051-1057, 1998.

46. **Schwartz AR, Smith PL, Wise RA, Bankman I and Permutt S**. Effect of positive nasal pressure on upper airway pressure-flow relationships. *J Appl Physiol* 66: 1626-1634, 1989.

47. **Schwartz AR, Smith PL, Wise RA, Gold AR and Permutt S**. Induction of upper airway occlusion in sleeping individuals with subatmospheric nasal pressure. *J Appl Physiol* 64: 535-542, 1988.

48. **Schwartz AR, Thut D, Roach D and Smith PL**. Effect of hypoglossal nerve stimulation on airflow mechanics in the isolated upper airway. *Am Rev Respir Dis* 143: A405, 1991.

49. **Schwartz AR, Thut DC, Brower RG, Gauda EB, Roach D, Permutt S and Smith PL**. Modulation of maximal inspiratory airflow by neuromuscular activity: effect of CO2. *J Appl Physiol* 74: 1597-1605, 1993.

50. **Schwartz AR, Thut DC, Russ B, Seelagy M, Yuan X, Brower RG, Permutt S, Wise RA and Smith PL**. Effect of electrical stimulation of the hypoglossal nerve on airflow mechanics in the isolated upper airway. *Am Rev Respir Dis* 147: 1144-1150, 1993.

51. **Seelagy MM, Schwartz AR, Russ DB, King ED, Wise RA and Smith PL**. Reflex modulation of airflow dynamics through the upper airway. *J Appl Physiol* 76: 2692-2700, 1994.

52. **Shahar E, Whitney CW, Redline S, Lee ET, Newman AB, Javier NF, O'Connor GT, Boland LL, Schwartz JE and Samet JM**. Sleep-disordered breathing and

cardiovascular disease: cross-sectional results of the Sleep Heart Health Study. *Am J Respir Crit Care Med* 163: 19-25, 2001.

53. **Smith PL, Wise RA, Gold AR, Schwartz AR and Permutt S**. Upper airway pressure-flow relationships in obstructive sleep apnea. *J Appl Physiol* 64: 789-795, 1988.

54. **Thut DC, Schwartz AR, Roach D, Wise RA, Permutt S and Smith PL**. Tracheal and neck position influence upper airway airflow dynamics by altering airway length. *J Appl Physiol* 75: 2084-2090, 1993.

55. **Van de Graaff WB**. Thoracic influence on upper airway patency. *J Appl Physiol* 65: 2124-2131, 1988.

56. **Van de Graaff WB**. Thoracic traction on the trachea: mechanisms and magnitude. *J Appl Physiol* 70: 1328-1336, 1991.

57. **Van Lunteren E, Haxhiu MA and Cherniack NS**. Effects of tracheal airway occlusion on hyoid muscle length and upper airway volume. *J Appl Physiol* 67: 2296-2302, 1989.

58. **Veasey SC, Chachkes J, Fenik P and Hendricks JC**. The effects of ondansetron on sleep-disordered breathing in the English bulldog. *Sleep* 24: 155-160, 2001.

59. **Watanabe T, Isono S, Tanaka A, Tanzawa H and Nishino T**. Contribution of body habitus and craniofacial characteristics to segmental closing pressures of the passive

pharynx in patients with sleep-disordered breathing. *Am J Respir Crit Care Med* 165: 260-265, 2002.

60. **Younes M**. Contributions of upper airway mechanics and control mechanisms to severity of obstructive apnea. *Am J Respir Crit Care Med* 168: 645-658, 2003.

61. **Young T, Peppard PE and Gottlieb DJ**. Epidemiology of obstructive sleep apnea: a population health perspective. *Am J Respir Crit Care Med* 165: 1217-1239, 2002.

Table 1. Effects of Positive End-Expiratory Pressure (PEEP) on passive upper airway characteristics (Pcrit and R_{US})

	PEEP Level (cmH_2O)			
Variable	**0**	**5**	**10**	**Mean ± SE**
P_{CRIT} ± SE (cmH_2O)	-6.93 ± 1.07	-6.92 ± 1.23	-6.53 ± 1.16	-6.79 ± 0.62
R_{US} ± SE (cmH_2O/ml/s)	14.4 ± 3.6	13.8 ± 3.0	14.4 ± 3.6	13.8 ± 1.8

FIGURE LEGENDS

Figure 1: Experimental set-up. The upper airway was isolated by bisecting the trachea. The nasal and tracheal ends of the upper airway were cannulated. The rostral trachea was connected to a negative pressure source and the caudal segment was connected to a ventilator (~). A pneumotach was placed in-line with the nasal cannula to measure airflow through the isolated upper airway. The pressures upstream (nasal) and downstream (tracheal) to the isolated upper airway (P_{US} and P_{DS}) were monitored, as was the tracheal pressure (P_{TRACH}) in the lower airway.

Figure 2: Representative recordings from one mouse illustrating the effects of three levels of upstream (nasal) pressure (P_{US}) and positive end-expiratory pressure (PEEP) on airflow ($V_I$max) through the isolated flow-limited upper airway. In each panel, positive pressure ventilation is delivered (see positive swings in tracheal pressure, P_{TRACH}, on left), and then abruptly discontinued, leading to a prolonged central apnea (spontaneous P_{TRACH} swings absent). During central apnea, PEEP was increased from 0 to 5 and 10 cmH_2O. $V_I$max decreased as P_{US} was lowered, but was not influenced by PEEP (the state of lung inflation). Note that phasic genioglossal EMG (EMG_{GG}) activity was absent, indicating suppression of central respiratory drive.

Figure 3: Representative passive pressure-flow relationship for the isolated upper airway at varying levels of lung inflation (positive end-expiratory pressure, PEEP) in the mouse illustrated in recording examples in Figure 2. A linear relationship between maximal inspiratory flow ($V_I$max) and upstream (nasal) pressure (P_{US}) was demonstrated from which the critical pressure

(Pcrit, -5.9 cmH_2O) and upstream resistance (R_{US}, 4.9 $cmH_2O/mL/s$) were derived. PEEP did not influence Pcrit or R_{US} significantly.

Figure 4: Time dependent upper airway flow and genioglossal EMG responses to tracheal occlusion at upstream (nasal) pressures of -4.0 (left panel) and 0.0 (right panel) cmH_2O. In each panel, the trachea was occluded following the discontinuation of positive pressure ventilation (see positive P_{TRACH} swings, left). After a period of central apnea, spontaneous breathing efforts resumed at the onset of the run (t_O) and increased progressively through the end of the run (t_f). Phasic levels of airflow through the isolated upper airway ($V_I$max) and raw genioglossal electromyographic activity (EMG_{GG}) increased progressively during the run. Phasic (open symbols) and tonic (closed symbols) EMG_{GG} and $V_I$max are illustrated in bottom graphs at bottom. While the phasic EMG_{GG} increased similarly at low and high nasal pressures, phasic increases in $V_I$max were markedly attenuated at the high compared to low nasal pressure (see lower left vs. right panels).

Figure 5: Effect of tracheal occlusion on phasic airflow ($V_I$max) and genioglossal electromyographic activity (EMG_{GG}). Group mean ($\pm$SE) phasic increases in upper airway flow (ΔV_Imax) vs. genioglossal electromyographic activity (ΔEMG_{GG}) are plotted for the highest (closed symbols) and lowest (open symbols) levels of nasal pressure applied (Low P_{US}: -3.4±1.1; High P_{US}: 5.7± 0.6 cmH_2O). The phasic component of the EMG_{GG} response to tracheal occlusion is represented at the start (lower left symbols) and end (right-most symbols) of the runs by subtracting the tonic level at the onset of the run from the peak phasic EMG_{GG} at each time point. Increases in ΔEMG_{GG} over the course of the runs were only associated with a significant increase in ΔV_Imax at low but not high levels of upstream nasal pressure ($p<0.0001$).

Figure 6: Passive and active pressure-flow relationships derived from representative recordings illustrated in Figure 4. The passive curve demonstrated a passive Pcrit of -4.2 cm H_2O. Tracheal occlusion resulted in phasic increases in $V_I$max, particularly at low P_{US} levels, and an overall reduction in slope of the active curve. The pressure difference, ΔP_{A-P}, between active and passive curves at passive Pcrit represents the strength of neuromuscular activation. See text for details.

Figure 7: The critical pressure (Pcrit) and upstream resistance (R_{US}) are represented for passive condition and for the active condition during inspiration and expiration. Pcrit was significantly lower in the active condition during inspiration than expiration ($p<0.005$) and was significantly lower than the passive Pcrit ($p<0.0005$). R_{US} was significantly higher in the active condition during inspiration than expiration ($p=0.011$) and was significantly higher than the passive R_{US} ($p<0.025$).

Figure 8: "Tube in box" model of upper airway and boney enclosure at low (left panels) and high (right panels) upstream pressures in active (lower panels) and passive (upper panels) conditions (see arrows representing dilator muscle action, active conditions). In passive condition, the airway is occluded at low and open at high upstream pressure. In active condition, dilator muscle activity improves airway patency (reduces its collapsibility) at the low but not high upstream pressure. Dilators restore patency at low upstream pressure in active condition because muscles are operating from optimal length in passive condition (L_O). Alternatively, patency does not improve at high upstream pressure because distension of the tube is limited by the size of the boney enclosure (box) when dilators contract.

Figure 1: Experimental Set-up

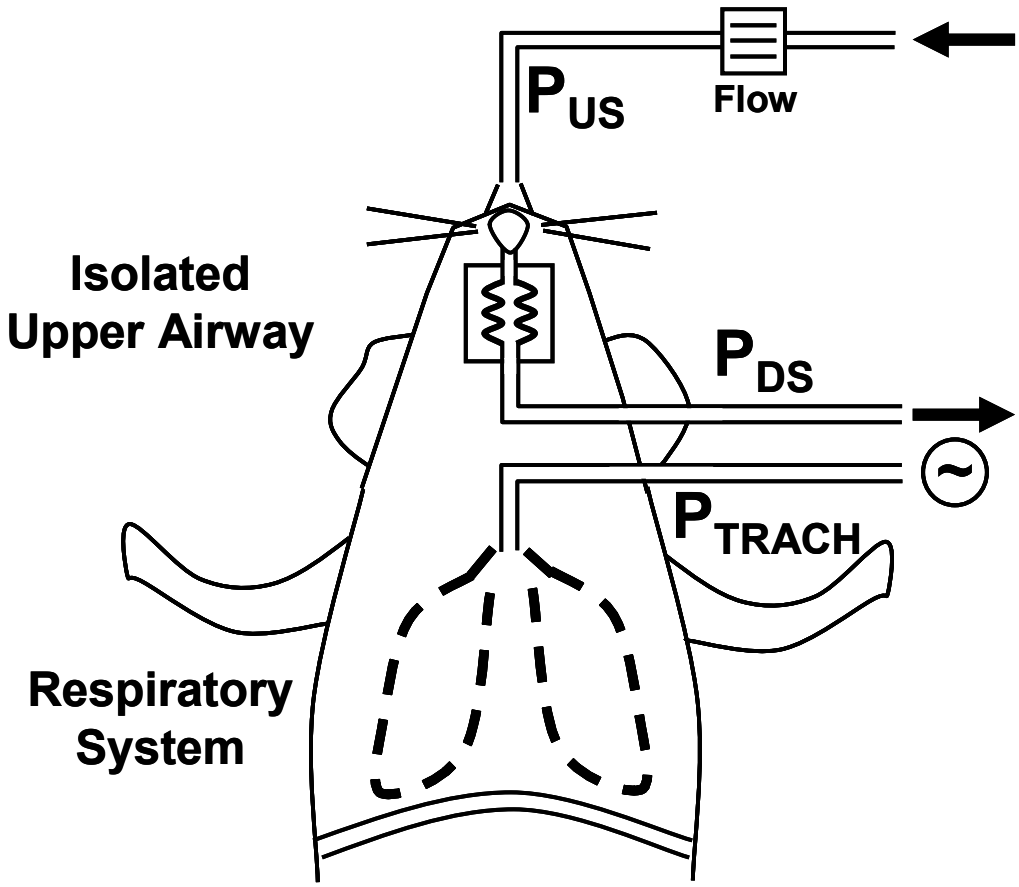

Figure 2: Representative recordings under passive condition at three levels of upstream pressure (P_{US}) and Positive End-Expiratory Pressure (PEEP)

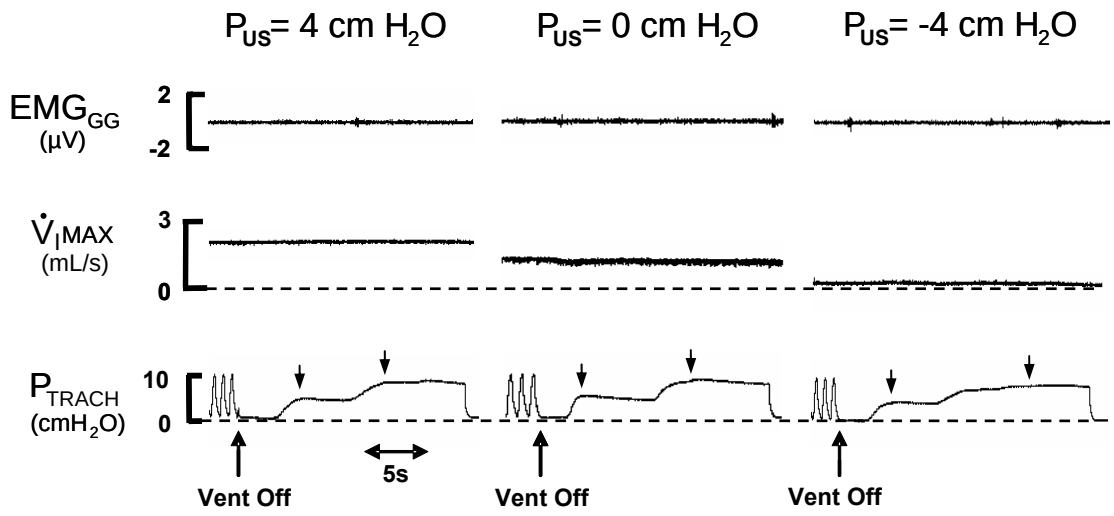

Figure 3: Passive $V_I$max vs. P_{US} relationship at several levels of positive end-expiratory pressure (PEEP)

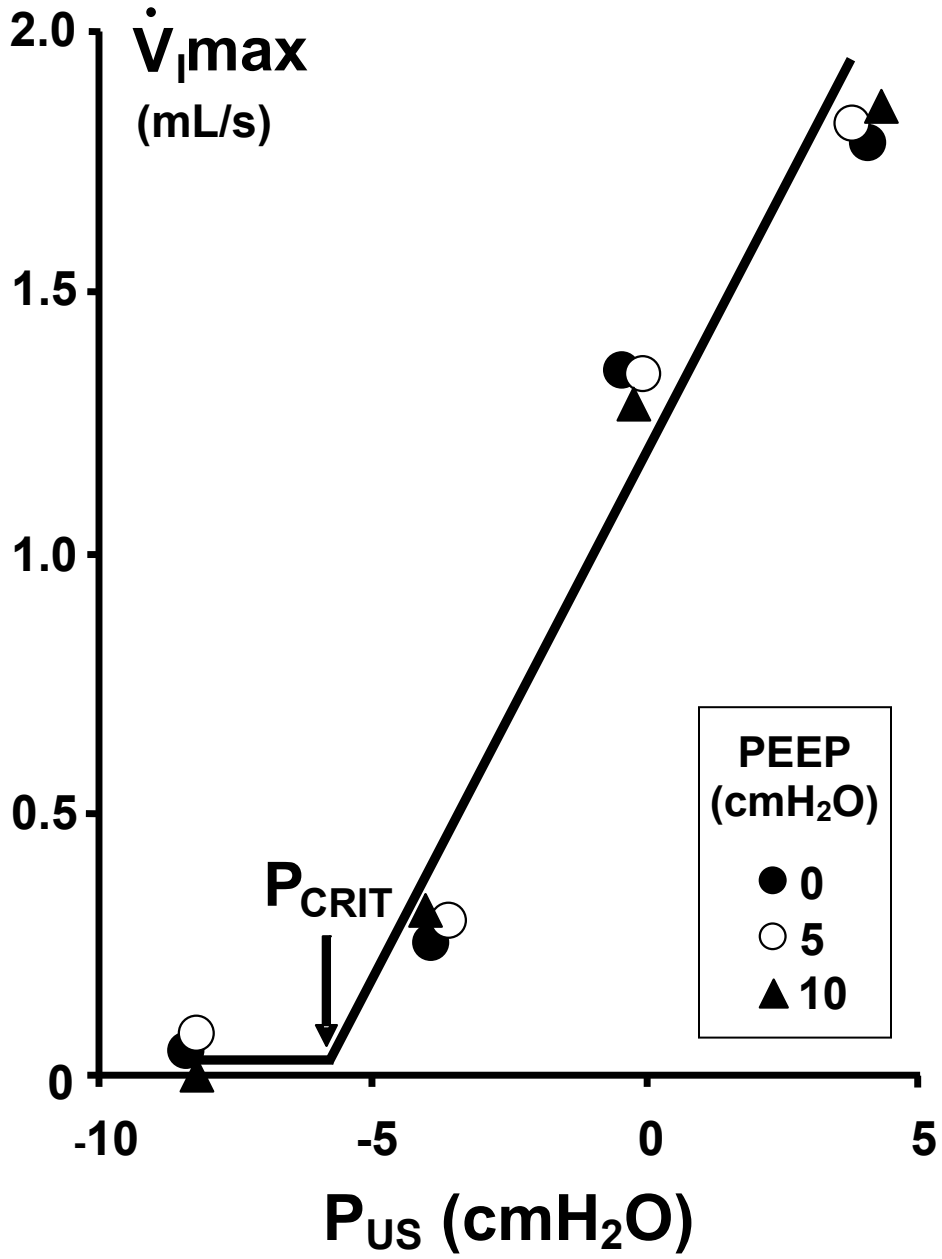

Figure 4: Representative recordings of active genioglossal EMG (EMG_{GG}) and airflow ($V_I max$) responses to tracheal occlusion at low and high upstream nasal pressure levels (P_{US})

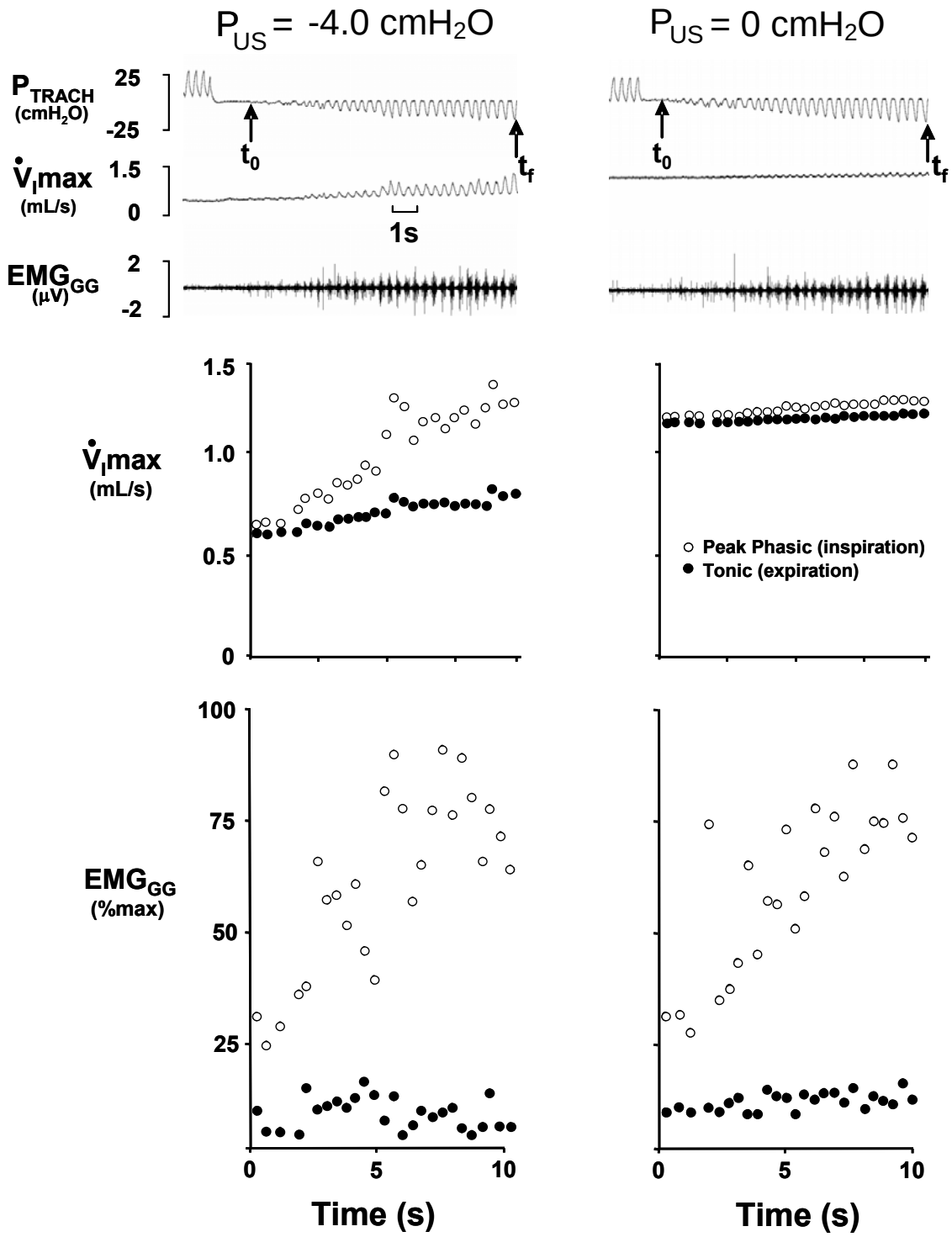

Figure 5: Phasic changes in airflow ($\Delta V_I max$) and genioglossal EMG (ΔEMG_{GG}) in response to tracheal occlusion at high and low upstream pressures (P_{US})

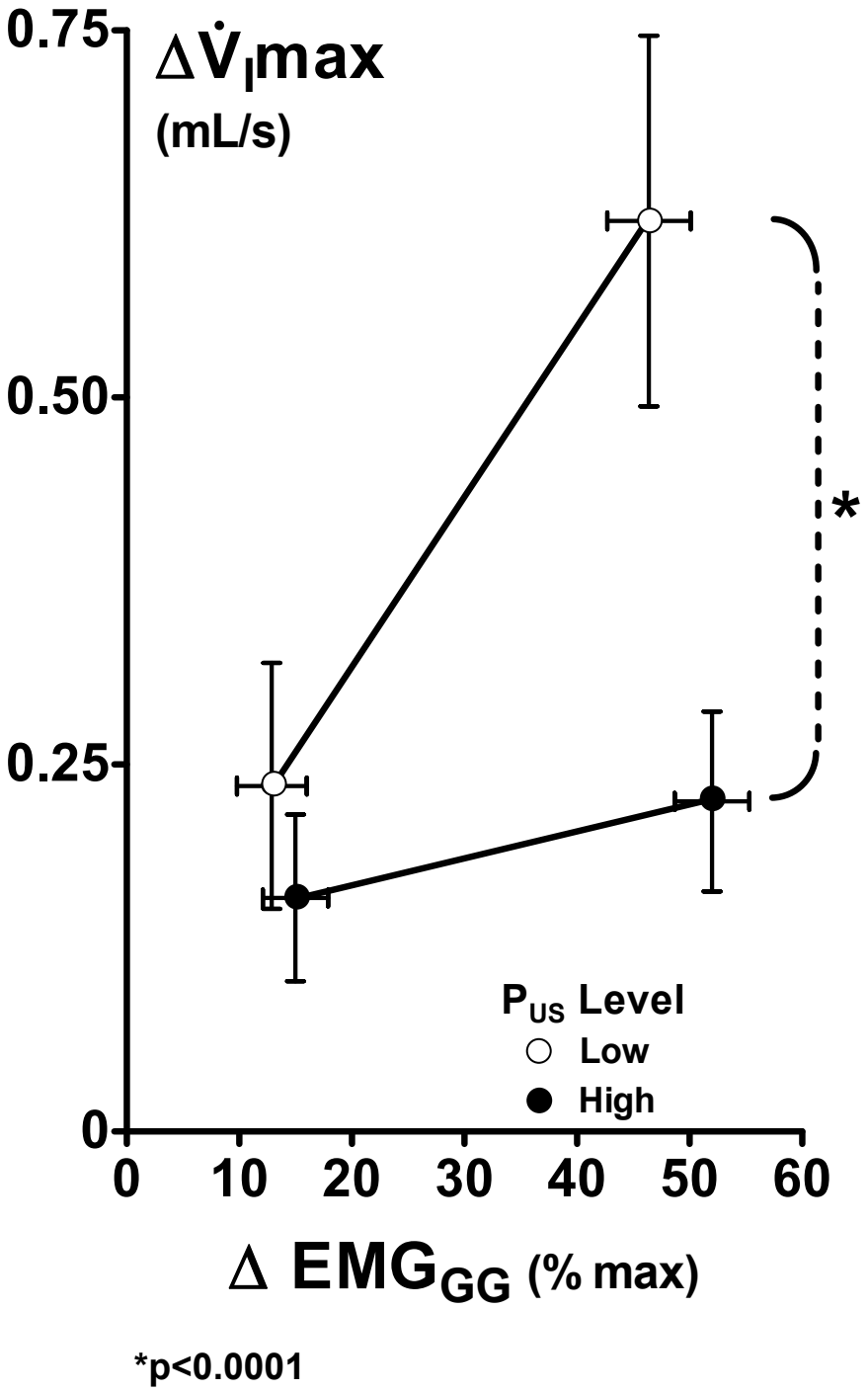

Figure 6: Active and passive $V_I$max vs. P_{US} relationship from pressure-flow recordings in Figure 4. See text for details.

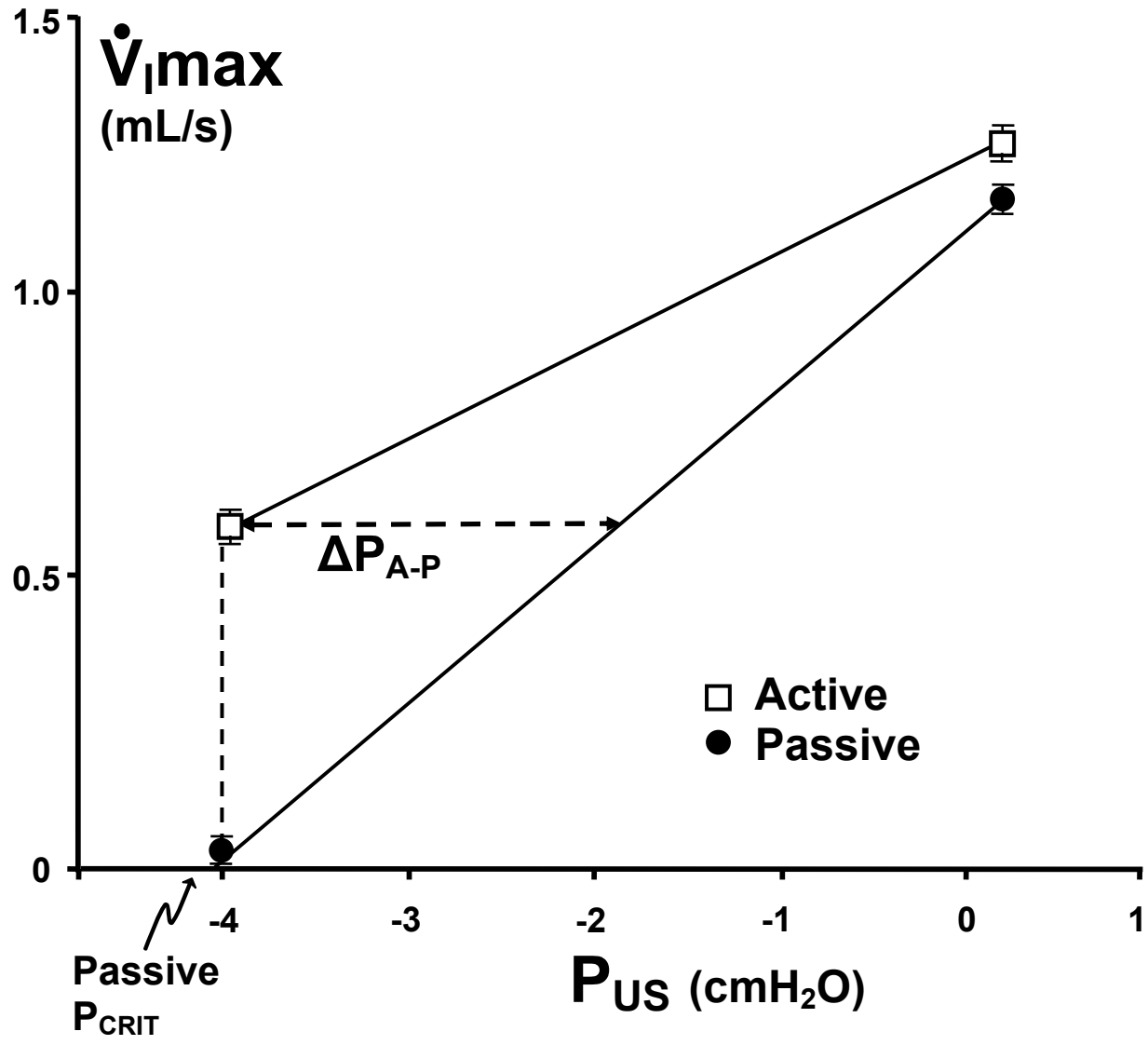

Figure 7: Passive and Active Pcrit (Left Panel) and Rus (Right Panel)

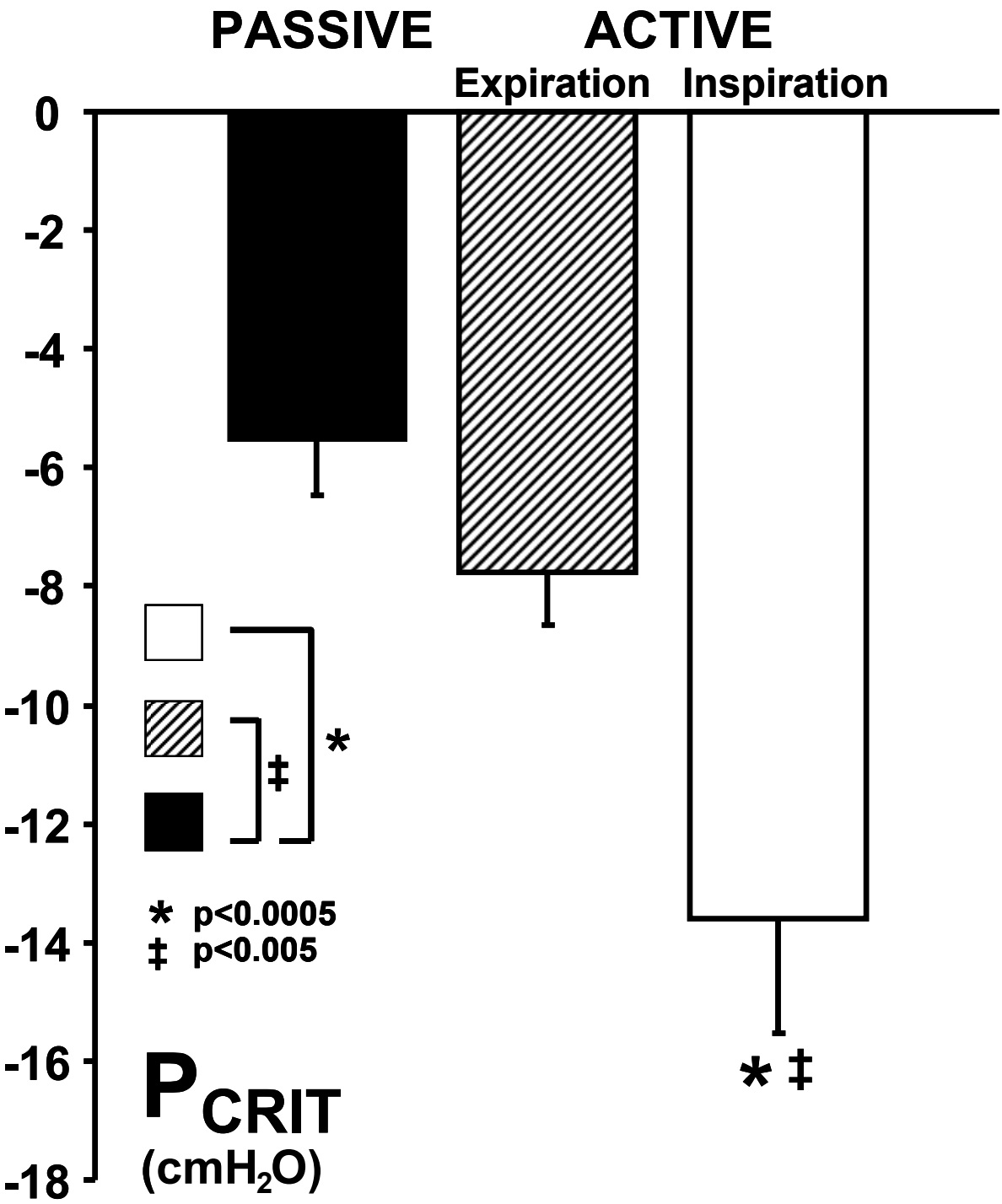

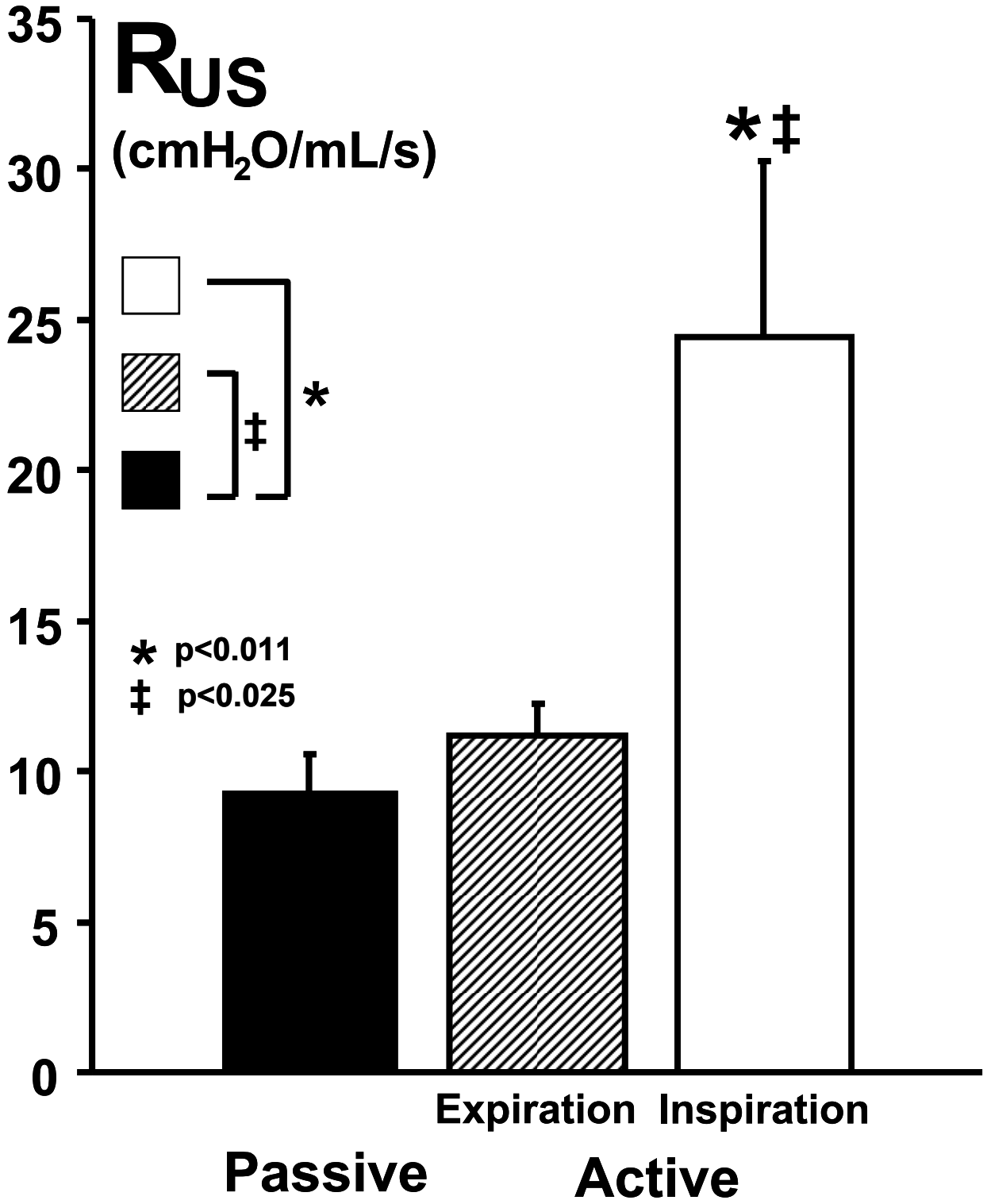

Figure 8: Upper Airway "Tube in Box" Model at two levels of upstream pressure (P_{US}) in passive and active conditions